Adaptive Load Control of Flexible Aircraft Wings Using Fiber Optic Sensing

Francisco Pena[1], Benjamin Martins[2], and W. Lance Richards[3]

Introduction

Over the past century aircraft wing design has transformed from the morphing wing used on the Wright Flyer to rigid wings with little to no shape-tailoring abilities. Modern day wings are designed to fly at a single trim condition and optimized to have a maximum aerodynamic efficiency at only this condition. Shape morphing wings on the other hand have the potential to undergo geometric changes allowing them to adapt to their mission profiles (ref. 1). Several flight demonstrations have been conducted over the decades using morphing-wing technologies, (ref. 2). Active wing-twist control was demonstrated on the X-53 Active Aeroelastic Wing (AAW) research project by utilizing multiple leading- and trailing-edge control surfaces (ref. 3). Passive morphing technology has been demonstrated on the Rockwell RPRV-870 Highly Maneuverable Aircraft Technology (HiMAT) aircraft. (Ref. 4)

In the current study, the wings of a small unmanned aerial system (sUAS) were modified to have segmented control surfaces (SCS). The modifications include segmenting the original wing control surfaces (one flap and one aileron per wing) into 44 individual sections, each section having its own independent servo control motor. The wings were also instrumented with a network of over 1800 fiber-optic strain sensors (on four sensing fibers distributed over the top and bottom surfaces of the wing) monitoring the strain response of the wing to aerodynamic loading. The SCS positions were manipulated in real time to modify the spanwise lift distribution of the wings on the sUAS. The change in the structural response of the wings caused by load redistribution was quantified by measuring the bending strains on the upper and lower wing surfaces using an on-board compact fiber-optic strain sensing (cFOSS) system. A feedback controller was developed to control the SCS positions using strain-based shape estimations from the Displacement Transfer Function (DTF) (ref. 5). Post-processing of the strain data allowed for the transverse displacement distributions and load distributions to be compared for the conventional and segmented control surface cases using displacements and loads algorithms developed by Richards and Ko at AFRC (refs. 5-10). While the current study focused on the shifting of the spanwise aerodynamic loads as quantified by displacements, future applications for loads or displacement control might include active gust alleviation and flutter suppression.

The Aircraft Testbed and Systems

The RnR Products (Milpitas, California) Alternatively Piloted Vehicle 3 (APV-3) testbed, shown in figure 1, was comprised of four major components: (1) a commercial-off-the-shelf 12.33-ft-wingspan unmanned aircraft, (2) a distributed fiber-optic strain sensor network and interrogation system, (3) SCS wings, and (4) SCS control hardware.

Figure 1. The stock APV-3 aircraft used for experiments on Rogers Dry Lake in Edwards, California.

Fiber-Optic Strain Sensors and Compact Fiber-Optic Strain Sensing System

Figure 2 provides a top view of the right wing instrumentation. The strain state of the wings was monitored using

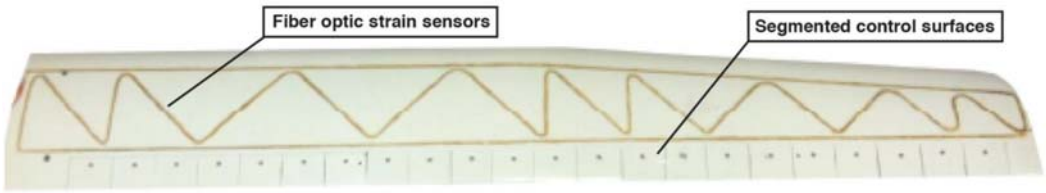

Figure 2. Upper surface of the modified right wing of the APV-3 aircraft after implementation of the fiber-optic strain sensors and segmented control surfaces.

[1] Armstrong Flight Research Center, Edwards, California,
[2] University of California, San Diego, San Diego, California
[3] Langley Research Center, Hampton, Virginia

continuous Bragg-grated fiber-optic strain sensors manufactured by FBGS Technologies GmbH (Jena, Germany). The optical fibers had a nominal diameter of 0.005 in and a linear weight of 0.00102 lb/ft. The upper and lower surfaces of each wing were instrumented with approximately 18 ft of fiber, per wing, per side, for a total of 74 ft of sensing fiber. The continuous Bragg-grated fiber-optic strain sensors were coupled with a cFOSS system developed at AFRC in order to obtain and process the strain data. The cFOSS system is approximately 12 in long, 6 in wide, and 6 in tall, with a nominal weight of 5 lb. The APV-3 aircraft was modified to have a vibration-isolation mounting system incorporated into its payload canoe whereby the cFOSS system was mounted. The system was set so that individual axial strains were measured at .50-in intervals along the length of the sensing fiber, providing more than 1800 distributed point strain measurements. The onboard computer within the cFOSS system was also able to process the distributed strain data to obtain an estimation of the transverse displacement of the wing in real time (utilizing the Displacement Transfer Function, reference 9). This transverse displacement was used as an input to the developed proportional feedback controller. In addition to interrogating the fibers and calculating strain and displacement from the collected optical information, the cFOSS system also functioned as a data logger, recording the time histories of each strain sensor to allow for post-flight processing.

Segmented Control Surfaces

The original wing control surfaces on the APV-3 aircraft were comprised of a 36-in flap and a 30-in aileron per wing. These control surfaces were segmented into 44 controls surfaces by sectioning the four control surfaces into 44 three-inch-wide control surfaces, 22 of which are shown on the right wing in figure 2 and figure 3. Each segment was independently controlled by a dedicated HiTec HS-82MG servo (HITEC RCD USA, Poway, California). Figure 3 shows the lower surface of the right wing with the SCS, servos, servo linkages and fiber-optic strain sensors.

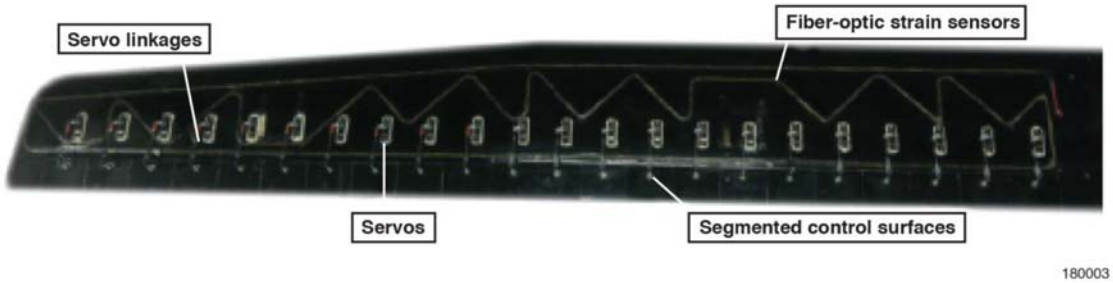

Figure 3 Lower surface of the modified right wing showing the segmented control surfaces, control servos, servo linkages, and fiber-optic sensors.

Segmented Control Surfaces Control Hardware and Architecture

To accompany the implementation of the 44 SCS onto the wings of the APV-3 aircraft, the hardware architecture responsible for controlling the wing servos had to be redesigned to handle the complex task of quickly and reliably controlling the 44 servos in unison. The control architecture for the SCS was designed such that the segments could not only be individually controlled but could also be controlled in sets to mimic the behavior of the stock (conventional) four control surfaces. The result of the segmented wings and control system was the ability of the APV-3 aircraft to monitor its wing displacements states and adjust this displacement profile (load distribution) to track a target value in real time.

Flight-Testing

Flight tests were conducted on Rogers Dry Lake on Edwards Air force Base (Edwards, California). Figures 4(a) and 14(b) provide images of the modified APV-3 aircraft during pre-flight checks on Rogers Dry Lake. Figure 4(c) shows the fully-modified APV-3 in flight.

Figure 4. (a) Pre-flight checks of the cFOSS system and the SCS control system during one of the work-up flights, (b) complete systems ground test prior to flight, and (c) fully-modified APV-3 in flight.

Each flight test consisted of a number of flight maneuvers, comparing SCS configurations with a conventional control surface configuration called the mimicked conventional control surface (MCCS). The MCCS allowed the structural performance of conventional and segmented control surface wings to be studied for comparable flight conditions. The test-point flight cards for each configuration contained a series of steady-level circuits, pitch doublets, roll doublets, and high-g steady turns.

Results

The results of the flight tests were compared over a range of maneuvers encompassing the entire flight plan. The strain distributions along the bottom surface of the right wing for the MCCS and SCS are presented in figure 5. The conventional configuration is plotted in purple; the SCS configuration is plotted in blue. Both the MCCS configuration and the SCS are normalized relative to the g-loading during the event as measured by the flight computer. During the load redistribution, the normalized root strain was reduced by approximately 30 percent (687 με/g to 476 με/g).

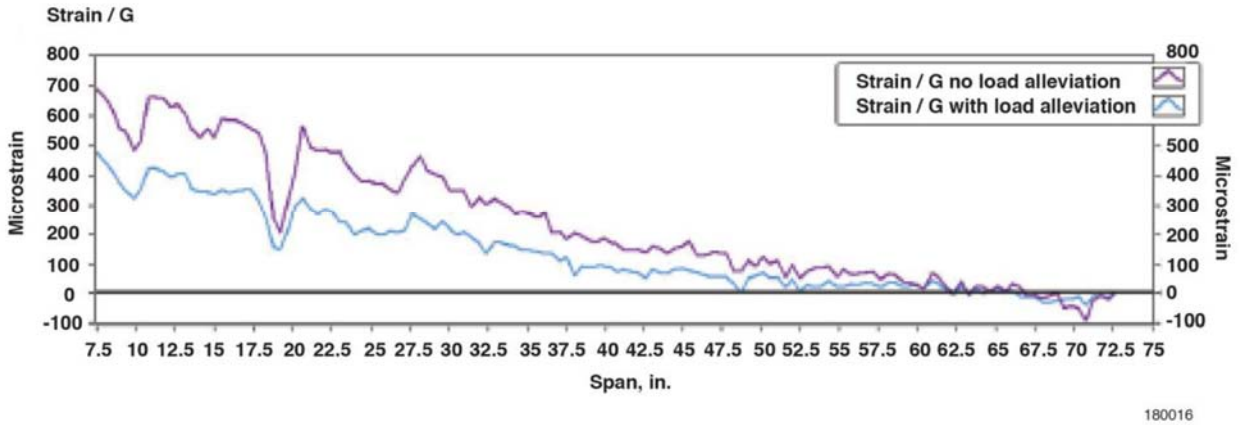

Figure 5. Normalized spanwise strain for the MCCS configuration (purple) and the SCC configuration (blue).

The deflections along the span of the right wing as calculated by the DTF are presented in figure 6. The conventional configuration is plotted in purple; the SCS configuration is plotted in blue. Both the configurations are normalized relative to the g-loading during similar flight conditions. During the load redistribution, the normalized tip-deflection was reduced by 38 percent (1.74 in/g to 1.07 in/g) when the control surfaces were fully deflected.

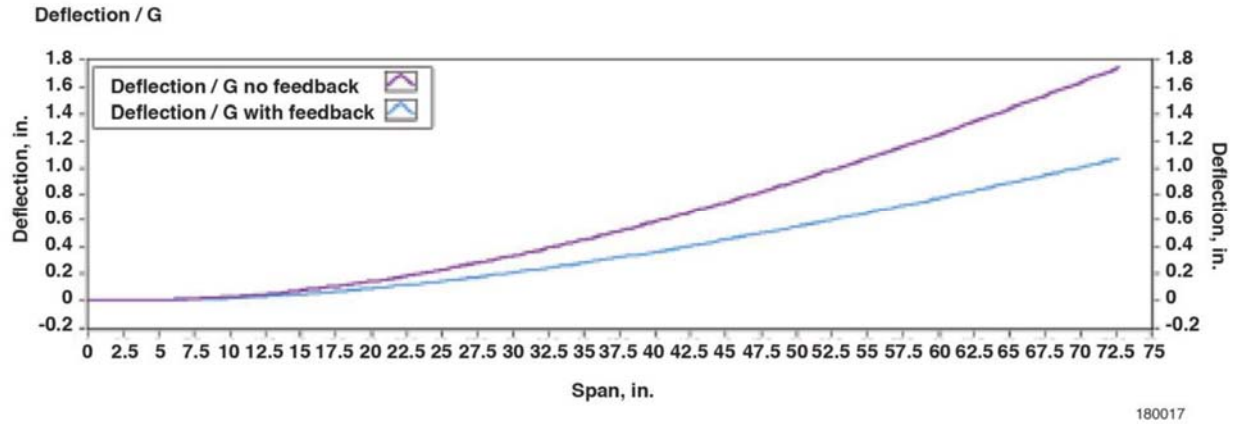

Figure 6. Normalized spanwise deflection during the flight for the MCCS (purple) configuration and the SCS (blue) configuration.

When the SCS algorithm was turned on it was observed that the normalized wing-tip displacement was lowered across all of the flight conditions, as was desired. The average vertical deflection while the SCS configuration was active was 1.22 in/g. A plot of tip deflection versus vertical acceleration for the MCCS and SCS configuration is provided in figure 7. In figure 7 it can be seen that the relationship between vertical tip deflection and vertical acceleration is relatively linear for the MCCS configuration, with an estimated 1.25-in deflection per unit g of vertical acceleration plus an offset of 0.64-in deflection. While the SCS algorithm was active, the vertical deflection per unit of vertical g force was reduced by an average of 0.67 in.

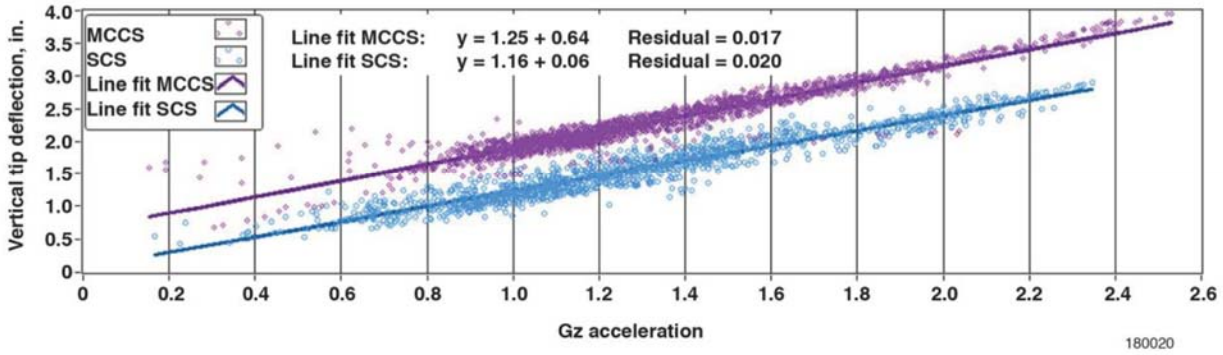

Figure 7. Vertical tip deflection (inches) versus vertical acceleration (g's) for the MCCS and the SCS.

Conclusion

An in-flight assessment of methodologies and techniques aimed at load redistribution and active shape control was performed. A conventional uninhabited aerial vehicle was modified to have 44 control surface segments and over 1800 points of strain measurement on the wings. The compact fiber-optic strain sensing (cFOSS) system developed at the NASA Armstrong Flight Research Center (AFRC) (Edwards, California) was utilized to measure in-flight strains and calculate the transverse deflection profile in real time using the patented Displacement Transfer Function developed at AFRC. A control algorithm was developed which utilized the current displacement profile and a 1-g reference profile to drive the deflection of the control surface segments in flight in real time. The implication of these results are that future structures which incorporate load redistribution or shape morphing technologies, or both, might withstand high loading events with reduced structural weight while maintaining acceptable margins. Increased control speed would also allow suppression of dynamic events such as flutter or wind gust. As well, the same system utilized for the displacement calculation and feedback control, the compact fiber-optic strain sensing (cFOSS) system, could further serve as a structural-health-monitoring system, ensuring the vehicle remains safe while optimizing the aerodynamic configuration.

References

1. Sofla, A. Y. N., S. A. Meguid, K. T. Tan, and W. K. Yeo, "Shape Morphing of Aircraft wing: Status and Challenges," Materials & Design, vol. 31, no. 3, pp. 1284-1292, DOI: 10.1016/j.matdes.2009.09.011.
2. Warwick, Graham, "Morphing Wings Are Still A Long Way From Reality," *Aviation Week & Space Technology,* January 8, 2016.
3. Pendleton, Edmund W., Denis Bessette, Peter B. Field, Gerald D. Miller, and Kenneth E. Griffin, "Active Aeroelastic Wing Flight Research Program: Technical Program and Model Analytical Development," Journal of Aircraft, vol. 37, no. 4, pp. 554-561, DOI: 10.2514/2.2654.
4. Monaghan, Richard C., *Description of the HiMAT Tailored Composite Structure and Laboratory Measured Vehicle Shape Under Load,* NASA-TM-81354, February 1981.
5. Ko, William L., W. Lance Richards, and Van T. Tran, *Displacement Theories for In-Flight Deformed Shape Predictions of Aerospace Structures,* NASA/TP-2007-214612, January 2007.
6. Jutte, Christine V., William L. Ko, Craig A. Stephens, John A. Bakalyar, W. Lance Richards, and Allen R. Parker, *Deformed Shape Calculation of a Full-Scale Wing Using Fiber Optic Strain Data from a Ground Loads Test,* NASA/TP-2011-215975, December 2011.
7. Bakalyar, John, and Christine Jutte, "Validation Tests of Fiber Optic Strain-Based Operational Shape and Load Measurements," AIAA-2012-1904, April 2012.
8. Ko, William L., W. Lance Richards, and Van Tran Fleischer, Applications of Ko Displacement Theory to the Deformed Shape Predictions of the Doubly-Tapered Ikhana Wing, NASA/TP-2009-214652, January 2009.
9. Ko, William L., and William Lance Richards, "Method for Real-time Structure Shape-Sensing," U.S. Patent No. 7,520,176 B1, issued April 21, 2009.
10. Richards, William Lance, and William L. Ko, "Process for Using Surface Strain Measurements to Obtain Operational Loads for Complex Structures," U.S. Patent No. 7,715,994 B1, issued May 11, 2010.